Microelectronic Engineering 194 (2018) 1–7

Contents lists available at ScienceDirect

Microelectronic Engineering

journal homepage: www.elsevier.com/locate/mee

Research paper

Polydimethylsiloxane films engineered for smart nanostructures

Tino Töpper *, Bekim Osmani, Bert Müller

Biomaterials Science Center, Department of Biomedical Engineering, University of Basel, 4123 Allschwil, Switzerland

ARTICLE INFO

Article history:
Received 13 October 2017
Received in revised form 16 February 2018
Accepted 26 February 2018
Available online 27 February 2018

Keywords:
(Sub-)micrometer-thin polymer membrane
Biomimetic film properties
Thermal expansion
Organic molecular beam deposition
Spectroscopic ellipsometry
Atomic force microscopy-based nano-indentation

ABSTRACT

Herein, we present organic molecular beam deposition to fabricate (sub-)micrometer-thin polydimethylsiloxane (PDMS) substrate-fixed films with a thickness homogeneity better than 2% on square centimeters. Their surface roughness and wrinkle morphology is controlled by the evaporation temperature, the growth rate, and the ultraviolet-light irradiation. The tailoring of the elastic modulus for the selected vinyl-functionalized PDMS nano-membranes is demonstrated. Both the surface morphology and mechanics are key parameters, which crucially determine the tissue-to-implant interactions for applications in bioelectronics. The cross-linked PDMS nano-membranes with elastic moduli of only a few hundred kPa are realized – a compliance similar to human soft tissues. The *in situ* characterization of their mechanical properties is presented based on their temperature sensitivity by spectroscopic ellipsometry and correlated to subsequently performed nano-indentation using a sophisticated atomic force microscopy instrument. Such soft sub-micrometer-thin elastomer membranes will become an essential component of dielectric elastomer transducers with strains comparable to human muscles, operated at the conventional battery voltages for future artificial muscles or skin implants.

1. Introduction

Flexible and foldable hetero-nanostructures based on silicone-based polymer materials provide access to nano-photonics [1,2], plasmonic biosensors [3], soft electronics [4–6] and dielectric elastomer nano-transducers (DET) [7]. Furthermore, their operation as bi-functional and self-sensing actuators is of relevance in flow control [8] or microfluidic devices [9]. As perspective low-voltage DET in medical applications, the reduction of the film thickness to the sub-micrometer range [7] or the use of high-permittivity polymers is required [10]. The nanometer-thin polymer and metal films can be fabricated using molecular beam deposition (MBD) – a versatile technique that leads reliably to homogeneous films with well-defined thickness [2,11,12]. *In situ* spectroscopic ellipsometry (SE) serves for the monitoring of the surface morphology of the growing film with sub-nanometer precision [2,13]. Because of its biocompatibility and the elastic properties, which can be very similar to human tissue [14], polydimethylsiloxane (PDMS) is used for a wide variety of medical implants [15]. The cross-linking of single PDMS chains is often achieved *via* ultraviolet light (UV) irradiation [7,16].

In the present study, we tailor the morphology of the (sub-)micrometer-thin PDMS films and manufacture dedicated wrinkles controlling the deposition rate and UV-irradiation. Moreover, the overall surface roughness of these films is influenced by the temperature in the crucible, which also determines the molecular weights of the molecules to be evaporated [11]. The same parameters of the film preparation process determine the elastic properties of the PDMS films. Three-dimensionally cross-linked PDMS networks are realized based on vinyl-functionalized PDMS. Atomic force microscopy (AFM)-based nano-indentation measurements on these (sub-)micrometer-thin membranes reveal an elastic modulus well below 1 MPa, a milestone to reach the elasticity of human soft tissues [14,17]. The nanometer precision of SE enables to resolve the temperature sensitivity of organic thin films to determine the thermal expansion coefficient (TEC) [18,19]. Correlated to the mechanical properties determined by AFM nano-indentations, we present the capability of SE to extract macroscopic elastic properties of the fabricated thin polydimethylsiloxane based on the generalized $E\alpha$ [2] relation.

The thickness homogeneity of soft polymer nano-membranes is essential to reliably operate low-voltage dielectric elastomer nano-transducers at strains as high as 10% while preventing an electrical breakdown [20]. As a medical implant, the device can operate as sensor, actuator, and energy harvester or any combination [7]. Therefore, the question arises how to control both the morphology of polymer membranes and their mechanical properties. We demonstrate that spectroscopic ellipsometry is a powerful technique to *on line* monitor the film thickness, the surface morphology as well as the elastic and thermal properties of the growing (sub-)micrometer-thin PDMS layers.

2. Materials and methods

2.1. Materials

The vinyl-terminated PDMS, *i.e.* DMS-V21 (Gelest Inc., Morrisville, PA, USA), was utilized as supplied. The average molecular weight was

* Corresponding author.
E-mail address: tino.toepper@unibas.ch (T. Töpper).

https://doi.org/10.1016/j.mee.2018.02.029

found to be 6000 g/mol with a polydispersity of 1.9 [11]. Two-inch Si (100)-wafers (SIEGERT WAFER GmbH, Aachen, Germany) with a thickness of (279 ± 25) μm were used as substrates. They are single-side polished and doped with boron.

2.2. Fabrication of (sub-)micrometer-thin PDMS films

The vacuum system consists of an ultra-high vacuum chamber (Vacom GmbH, Jena, Germany) with multiple evaporation sources. The base pressure of 10^{-9} mbar is realized by a pre-pump (Pfeiffer Duo Line, Pfeiffer, Asslar, Germany) and a turbo molecular pump (Turbo WAC MAG W600, Oerlikon Leybold Vacuum, Köln, Germany). DMS-V21 is thermally evaporated under vacuum conditions at a background pressure of 10^{-6} mbar from a low-temperature effusion cell (NTEZ, Dr. Eberl MBE Komponenten GmbH, Weil der Stadt, Germany) using a 25 cm^3 crucible. The temperature ramp of the effusion cell was adjusted to 10^{-2} K/s to avoid boiling retardation. The Si-substrate was held to a constant temperature of 293 K and set to a distance of 400 mm to the crucible. The rotation of the substrate was deactivated. The cross-linking of the vinyl-terminated DMS-V21 was promoted by *in situ* ultra-violet (UV) light irradiation from an externally mounted deuterium lamp (H2D2 light source L11798, Hamamatsu, Japan) through a CaF_2-window. The UV spectrum of the deuterium lamp exhibits a peak intensity at a wavelength of approximately 190 nm. The preferential pathway of vinyl-group radicalization is accompanied by methyl side group radicalization *via* UV irradiation for wavelengths below 170 nm. C—H and even Si—C bonds are radicalized and form linking sites for the three-dimensional cross-linking between the PDMS chains [7,21].

2.3. Spectroscopic ellipsometry

In order to monitor the changes of the optical properties and the increasing film thickness of the growing polymer, a spectroscopic ellipsometer (SE801, Sentech, Berlin, Germany) with SpectraRay3 software was applied. The spectroscopy-relevant angles Ψ and Δ were monitored for wavelengths between 190 and 1050 nm at an incident angle of 70° to the normal of the substrate's surface. The incident photon beam 4 mm in diameter resulted in a 4 × 10 mm^2 spot on the substrate, for which the average values were detected. The obtained Ψ- and Δ-values are related to the complex Fresnel reflection coefficients r_p and r_s of *p*- and *s*-polarized light and their ratio ρ by.

$$\rho = r_p/r_s = \tan\psi \cdot e^{i\Delta} \quad (1)$$

Based on the derived Fresnel reflection coefficient ratio it is possible to extract the wavelength-dependent dielectric function ε(λ) [13] of the growing PDMS films modeled with the Tauc-Lorentz (TL) dispersion [13]. A Bruggeman effective medium model [13] (EMA) served for the determination of the surface roughness. This layer is considered to have an effective dielectric or optical property deduced from equal fractional parts of deposited PDMS with refractive index n_i and n_e of the air, *cf.* Eq. (2):

$$0 = \sum_{i=1}^{N} f_i \frac{n_i^2 - n_e^2}{n_i^2 + 2n_e^2} \quad 2$$

The EMA is applicable, if two key assumptions are fulfilled. First, the features on the surface are smaller than the minimum wavelength to ignore light scattering. Second, the dielectric function is independent on the changes of the size and the shape of the features during growth. For data evaluation the void fraction was set to 0.5 [13]. For most of the thermally evaporated PDMS membranes, these assumptions can be regarded as fulfilled. For the membranes with a mean surface roughness above 10 nm, however, the TL-model can serve to simulate the scattering and leads to enhanced data conformity.

The mean square error (MSE), as the divergence of the obtained model fit to the acquired data, was calculated. The MSE is defined according to the figure of merit as

$$\mathrm{MSE} = \frac{1}{N}\sqrt{\sum_{i=1}^{N}\left\{\left(\frac{\psi_i^{\mathrm{mod}} - \psi_i^{\mathrm{exp}}}{\sigma_{\psi,i}^{\mathrm{exp}}}\right)\right\} + \left\{\left(\frac{\Delta_i^{\mathrm{mod}} - \Delta_i^{\mathrm{exp}}}{\sigma_{\psi,i}^{\mathrm{exp}}}\right)\right\}} \quad (3)$$

with the random and systematic error σ.

2.4. Atomic force microscopy

The surface topology of the thermally evaporated films was *ex situ* scanned using atomic force microscopy (FlexAFM C3000, Nanosurf AG, Switzerland). AFM scans were performed in tapping mode using a soft and long cantilever with a tip radius smaller than 10 nm (Tap190Al-G probe, NanoAndMore GmbH, Wetzlar, Germany) to minimize the deformation of the polymer membrane. 10 × 10 μm^2-regions of interest were scanned at a vibration amplitude of 424 nm and a set point of 60%. The root-mean-squares values were calculated using Gwyddion 2.41 software (Gwyddion: Open-source software for SPM data analysis, http://gwyddion.net). AFM nano-indentations were applied using cantilevers with spherical tips (R = (522 ± 4) nm, B500 FMR, Nanotools GmbH, Germany). The nominal spring constant of the cantilever, k = 2.6 Nm, was determined using the Sader method [22] and was found to be k = (2.6 ± 0.2) N/m. 400 nano-indentations on 10 × 10 μm^2 served for the calculation of the average elastic modulus. The elastic modulus of the membrane is related to the slope of the unloading force curve, which was fitted for each nano-indentation site along the entire backward indentation curve. The applied Johnson-Kendall-Roberts (JKR) model is implemented in the FLEXANA software (Nanosurf AG, Switzerland). This model takes into account the adhesion forces of the cantilever tip and the PDMS surface [23] and thus, is recommend as adequate contact model for soft and thin PDMS membranes [20,24].

3. Results

3.1. Surface morphology

Exemplarily, Fig. 1 shows the AFM images of the surface morphology for selected films with the thickness indicated. They were prepared by thermal evaporation during UV-irradiation. The valley-to-peak height difference increases from (3.6 ± 0.1) nm *via* (10.5 ± 0.2) nm to (82.5 ± 0.5) nm with the film thickness d. This result corresponds to an overall increase in root-mean-square (RMS) roughness on the 10 × 10 μm^2-areas from (0.5 ± 0.2) nm *via* (2.7 ± 0.4) nm to (11.6 ± 1.0) nm.

The impact of the growth rate on the surface structure is presented in the images of Fig. 2. The valley-to-peak height difference is found to be (9.2 ± 0.2), (17.5 ± 0.4) and (17.9 ± 0.5) nm for films grown at rates of 0.291, 0.163 and 0.073 μm/h, respectively. These values correspond to an increase in RMS roughness of (2.7 ± 0.4) nm to (6.0 ± 0.5) nm, see Fig. 2a/b. The further reduction of the growth rate to 0.073 μm/h does not show any significant roughness change, as the RMS roughness corresponded to (6.1 ± 0.5) nm. This surface, however, is wrinkled and shows a preferential orientation of the nanometer-size features, as the Fourier transform in Fig. 2c clearly demonstrates. The wavelength of these wrinkles corresponds to (195 ± 15) nm.

The diagram in Fig. 3a quantitatively displays the RMS roughness of the membranes as the function of the evaporation temperature using a dedicated color map from blue to red. A distinct increase of the surface roughness with film thickness is found for membranes fabricated at similar growth conditions, see Table 1. The data of membranes shown in Fig. 1 can be fitted using an exponential function: $RMS = (A + RMS_{\mathrm{Si}})\exp.(d/c) + A$, *cf.* dashed line in Fig. 3. The offset of minimal RMS roughness is given by the surface roughness of the Si-substrate RMS_{Si} = (0.15 ± 0.02) nm. With A = (2.32 ± 1.31) nm the growth

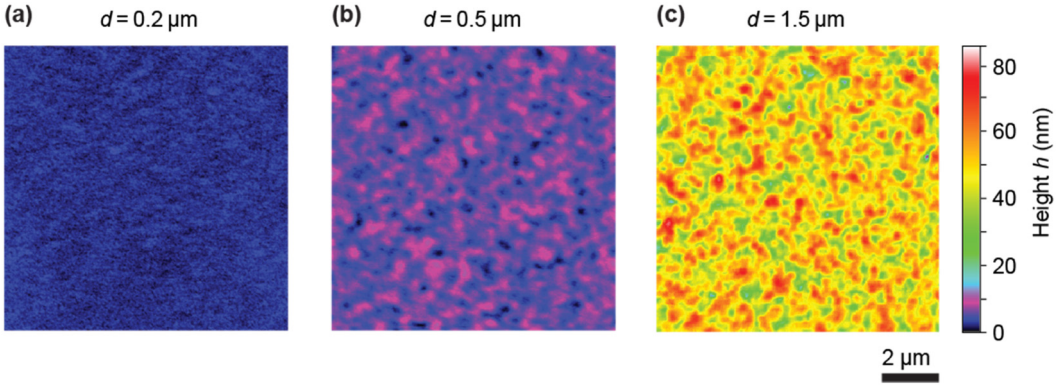

Fig. 1. Surface morphology of (sub-)micrometer-thin PDMS membranes prepared by thermal deposition under high-vacuum conditions and *in situ* UV light irradiation. The AFM scans show the characteristic morphology on an area of 10 × 10 µm² for PDMS films with thicknesses *d* of (a) 0.2 µm, (b) 0.5 µm, (c) and 1.5 µm. The surface roughness increases with the film thickness under *in situ* UV-irradiation with a power density of 0.6 µW cm^{-2} nm^{-1} at a wavelength of 190 nm.

constant *c* was extracted as (0.89 ± 0.21) µm^{-1}. Table 1 lists the RMS roughness together with the film thickness, the crucible temperature and the resulting growth rate *G* for the set of samples. The roughening of the surface is pronounced with decreasing evaporation temperature. Exemplarily, the RMS roughness increases from (1.4 ± 0.3) *via* (2.7 ± 0.4) to (6.0 ± 0.5) nm for the 0.5 µm-thin PDMS membranes grown at crucible temperatures of (260 ± 2), (230 ± 2) and (195 ± 2) °C, respectively.

The correlation of the surface roughness to the MBD parameters is displayed in Fig. 3b. The ratio of the RMS roughness and the film thickness depends on the molecular weight of the evaporated PDMS molecules, which is not only given by the molecular weight distribution of the PDMS in the crucible, but also essentially by the crucible temperature. Thus, the detected growth rate, represented by the color map, is dependent on the molecular weight distribution of the utilized prepolymer DMSV21 and the selected temperature of the evaporation source [11]. With increasing molecular weight of the PDMS molecules and increasing growth rate, the RMS roughness per grown micrometer film decreases.

3.2. Mechanical properties

Fig. 4a displays a diagram with the elastic moduli of the PDMS membranes for growth rates between 0.01 and 0.42 µm/h. Fig. 4b compares the histograms, *i.e.* the elastic modulus distribution detected on 0.2 µm-thin, 0.5 µm-thin, and 1.5 µm-thin films deposited at a growth rate of (0.25 ± 0.2) µm/h. The center of the elastic modulus distribution at (1.2 ± 0.4) MPa for a 1.5 µm-thin membrane is found to be 1.8 times smaller than the value of a 0.5 µm-thin membrane with (2.1 ± 0.4) MPa and nine times smaller compared to the 0.2 µm-thin membrane with (11.1 ± 0.4) MPa. It should be noted that a load of 200 nN was applied to the AFM cantilever in order to realize an indentation depth of about 100 nm for the three films. To this end, this stiffening effect is linked to substrate effects, which becomes more pronounced for thin films. In order to exclude this stiffening, most of the data were measured for 0.5 µm-thin membranes, see Fig. 4a. The applied loads were adjusted between 100 and 500 nN to realize an indentation depth of about 100 nm for the membranes with the elastic modulus ranging from (0.56 ± 0.15) to (150 ± 10) MPa. The higher the growth rate

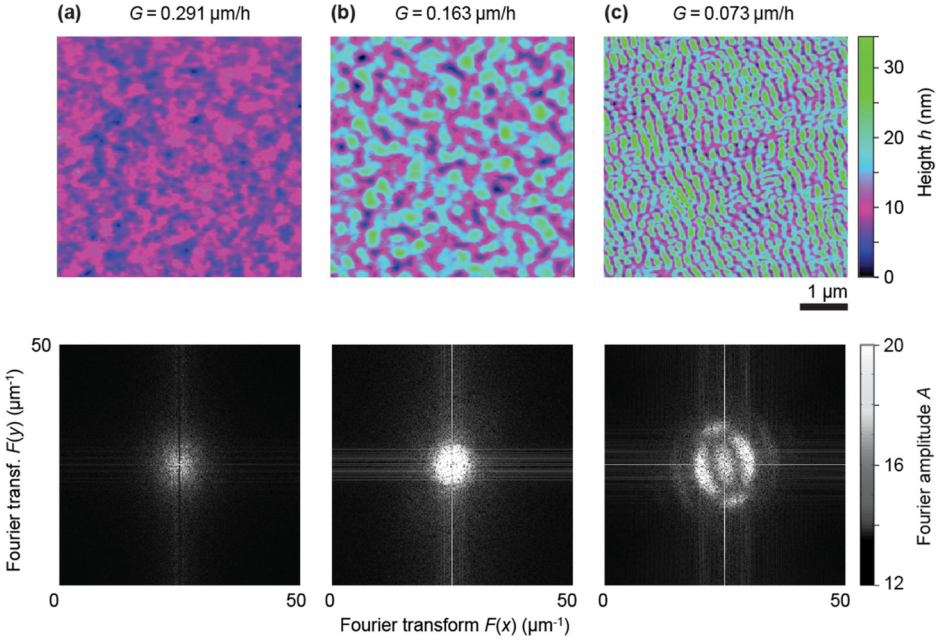

Fig. 2. Ordered nanostructures on (sub-)micrometer-thin PDMS membranes prepared by thermal deposition at increasing *in situ* UV-light irradiation dose. The AFM images cover a scanning area of 5 × 5 µm². The films were deposited at growth rates of (a) 0.291 µm/h, (b) 0.163 µm/h, and (c) 0.073 µm/h under *in situ* UV-irradiation with a power density of 0.6 µW cm^{-2} nm^{-1} at a wavelength of 190 nm. The lowest growth rate results in ordered nanostructures as demonstrated by the Fourier transforms of the images.

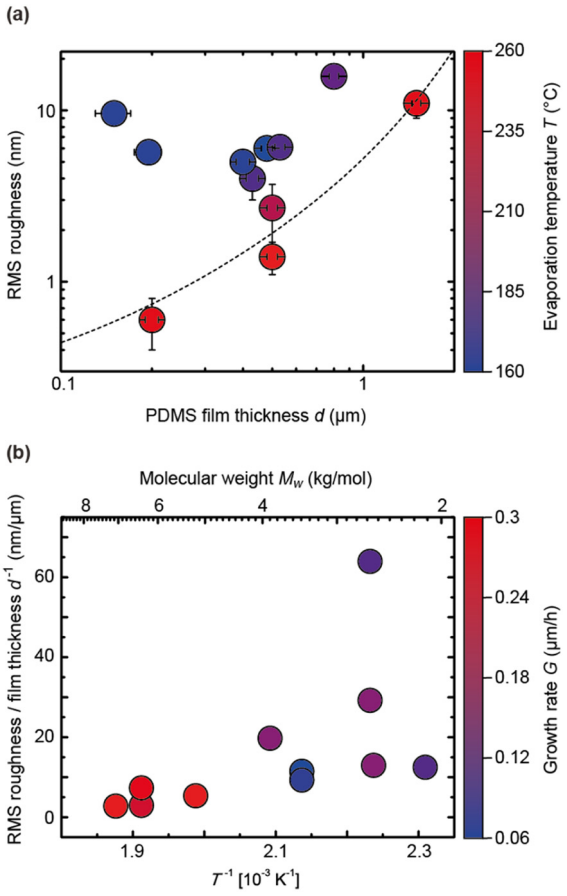

Fig. 3. The measured RMS roughness of (sub-)micrometer-thin PDMS membranes prepared by thermal deposition under *in situ* ultra-violet light irradiation. (a) Double-logarithmic plot presenting the RMS roughness of PDMS membranes with respect to the film thickness ranging from 0.2 to 1.5 μm and their evaporation temperature ranging from 160 to 260 °C (blue to red color map) under *in situ* UV light irradiation with a power density of 0.6 μW cm^{-2} nm^{-1} at a wavelength of 190 nm. The RMS roughness increases with the film thickness and decreasing evaporation temperature. The dashed lines correspond to an exponential fit to the three data points of the membranes presented in Fig. 1. The *y*-axis offset is correlated to the minimal RMS roughness RMS_{Si} = (0.15 ± 0.02) nm given by the Si-substrate. (b) The RMS roughness per grown micrometer of PDMS membranes d^{-1} is presented with respect to the inverse temperature T^{-1} (lower *x*-axis) and the corresponding average molecular weight of the evaporated PDMS molecules M_w (upper *x*-axis). The color map displays the growth rate *G* ranging from 0.06 to 0.30 μm/h (blue to red color). The RMS roughness per grown micrometer increases with decreasing evaporation temperature and decreasing evaporated average molecular weight.

and related crucible temperature the lower is the UV-light irradiation dose and the related elastic modulus of the PDMS film. Therefore, the lowest elastic modulus of (560 ± 150) kPa was obtained at the highest crucible temperature (230 °C) and growth rate (0.42 μm/h). An asymptotic exponential function allows for the extraction of a maximum elastic modulus of (608 ± 9) MPa, obtained at infinitely low growth rates.

3.3. Spectroscopic imaging ellipsometry

Spectroscopic ellipsometry reliably allows for the extraction of film thickness, morphology and dielectric properties of homogenous nanometer-thin heterostructures [2]. Based on AFM scans at step edges, the film thickness is measured with sub-nanometer resolution for verification purposes. Such a measurement is essential for the suitable modeling of the dielectric properties of the PDMS membranes to the measured Ψ - Δ data, see Fig. 5a. A set of 0.5 μm-thin membranes has been prepared by thermal evaporation and *in situ* UV-crosslinking. Changing the substrate temperature, the Δ-spectrum shifts to longer

Table 1
Surface morphology of (sub-)micrometer-thin PDMS membranes prepared by thermal deposition under *in situ* ultra-violet light irradiation. The RMS roughness extracted from AFM scans depicted in Figs. 1 and 2 are listed with respect to the evaporation temperature *T*, growth rate *G* and the final film thickness *d* of PDMS membranes prepared by thermal evaporation. The film thickness and the resulting growth rate including their errors were determined by *in situ* spectroscopic ellipsometry. The error of the RMS roughness arises from repetitive AFM scans over selected areas on the two-inch wafers.

Film thickness *d* (μm)	Evap. Temp. *T* (°C)	Growth rate *G* (μm/h)	RMS roughness (nm)	RMS/*d* (nm/μm)
0.15 ± 0.002	175 ± 2	0.150 ± 0.005	9.6 ± 0.2	64 ± 2
0.195 ± 0.004	175 ± 2	0.200 ± 0.005	5.7 ± 0.4	29.2 ± 1.3
0.2 ± 0.004	230 ± 2	0.250 ± 0.005	0.5 ± 0.2	2.0 ± 0.8
0.4 ± 0.01	175 ± 2	0.200 ± 0.005	5.0 ± 0.5	13.0 ± 1.3
0.43 ± 0.01	195 ± 2	0.110 ± 0.003	4.0 ± 0.3	9.3 ± 0.8
0.48 ± 0.015	195 ± 2	0.163 ± 0.006	6.0 ± 0.5	12.5 ± 1.1
0.5 ± 0.02	260 ± 2	0.280 ± 0.008	1.4 ± 0.3	2.8 ± 0.6
0.5 ± 0.02	230 ± 2	0.291 ± 0.012	2.7 ± 0.4	5.4 ± 0.7
0.53 ± 0.02	195 ± 2	0.073 ± 0.003	6.1 ± 0.5	11.5 ± 1.0
0.8 ± 0.024	205 ± 2	0.200 ± 0.006	15.8 ± 1.5	19.8 ± 1.8
1.5 ± 0.045	250 ± 2	0.270 ± 0.009	11.6 ± 1.0	7.3 ± 0.6

wavelengths, see diagram in Fig. 5b. The dielectric function of the polymer and the film thickness of the membrane are concurrent fitting parameters in the modeling of this shift. While the variation of the film thickness (Fig. 5d) can model the absolute shift of the Ψ - Δ spectra, the variation of the refractive index $n(\lambda)$ (Fig. 5c) enables to compress or stretch the Ψ - Δ spectra. A decrease of the refractive index, exemplary derived at a wavelength of 633 nm, and an increase in the film thickness with the substrate temperature was found. A polynomial fit of third order (red-colored line in Fig. 5d) can describe the thermal expansion $\Delta d/d$ of the PDMS membrane towards increased film thickness and decreased optical density based on the quadratic temperature dependency of thermal expansion coefficient α [25]. The thermal expansion is set as a linear function $\Delta d/d = \alpha(T) \times T - (0.089 \pm 0.008)$ with $\alpha = \alpha[293\ K] \times (1 + 3 \times 10^{-4}\, T + 3 \times 10^{-7}\, T^2)$ and $\alpha[293\ K] = (2.85 \pm 0.19)\ 10^{-4}\ K^{-1}$.

4. Discussion

The surface of PDMS membranes prepared by thermal evaporation and simultaneous UV-irradiation becomes rougher with increasing film thickness. The ratio between RMS roughness and film thickness, however, only depends on the evaporation temperature and the growth rate, as clearly demonstrated in Fig. 3b. Assuming, that the vinyl end-groups and the methyl side-groups of the PDMS molecules are already radicalized at arrival on the substrate, they can be directly incorporated into the formed PDMS network. Because of the strong intermolecular interactions between the methyl side groups [27], the mobility on the surface is limited. The increase of the crucible temperatures leads to an increase of the molecular weight of the evaporated molecules and an enhanced kinetic energy of the molecules hitting the substrate. Furthermore, at temperatures above 400 K, the molecules with more than 19 repeating units exhibit an enhanced folding flexibility [11]. This behavior indicates a smoothening of the surface with increasing evaporation temperature. Exemplarily, for 0.5 μm-thin membranes, the RMS roughness decreases by a factor of 3.5 for an evaporation temperature increase by 75 K from 195 °C (468 K) to 260 °C (533 K). This phenomenon is well known from heteroepitaxial growth of metals, where the surface roughness increases for lower and lower substrate temperatures [28].

Contrary to the evaporation of metals, however, the deposition rate of polymers is limited and depends on the thermal stability. In the present case, only molecules with an average molecular weight below about 6000 g/mol can be evaporated and the crucible temperature should not exceed 230 °C, a temperature we observe cross-linking in the crucible. This thermal boundary is given by the thermal stability of the functional

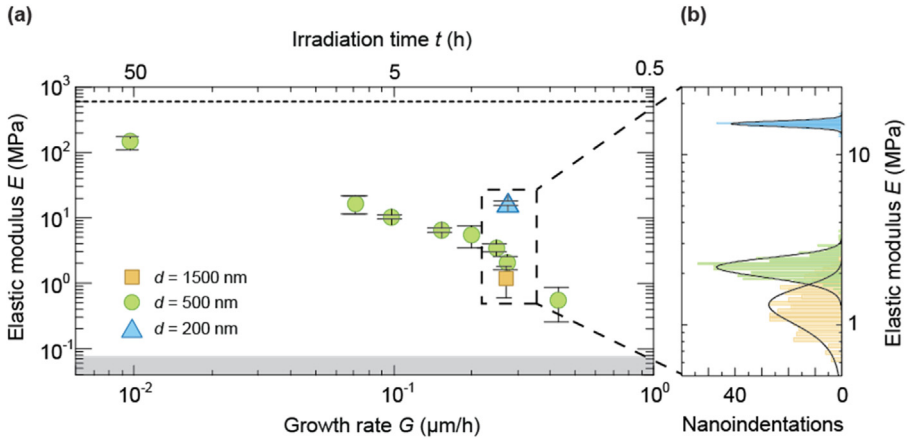

Fig. 4. The elasticity of the three-dimensionally cross-linked PDMS networks tailored *via* the growth rate and the irradiation dose. (a) AFM nano-indentations with a maximum load of 200 nN enabled us to determine the elastic properties of the (sub-)micrometer-thin PDMS membranes. The derived elastic modulus E is presented on a double-logarithmic plot for the selected growth rates G of thermally evaporated PDMS, cross-linked *via in situ* UV light irradiation using a deuterium lamp with a power density of 0.6 µW cm^{-2} nm^{-1} at a wavelength of 190 nm. At increasing growth rates, which corresponds to a decreased UV irradiation time and UV light dose, the elastic modulus of 0.5 µm-thin membranes decreases (green circles). The grey-shaded area characterizes the elastic modulus of 0.084 MPa measured by nano-indentations on a viscoelastic, incompletely cross-linked PDMS film [16]. The dashed line represents the maximal elastic modulus of (608 ± 9) MPa arising from an asymptotic fit to the data of 0.5 µm-thin membranes. (b) The diagram on the right compares the elastic modulus distribution detected on a 0.2 µm-thin (blue), 0.5 µm-thin (green) and 1.5 µm-thin (yellow) film fabricated at growth rates of 0.25 to 0.27 µm/h. The black lines represent the Gaussian fit allowing for the extraction of the amplitude and the full width at half maximum of the elastic modulus distribution.

vinyl end-groups [29]. A further temperature increase leads to the PDMS chain prolongation, which prevents evaporation [11].

It is important to mention that, contrary to the conventional growth, the increase of the growth rate does not result in rougher films. Instead, we observed a smoothening of the PDMS films with the growth rate associated with a decreased UV-irradiation power per PDMS molecule. Therefore, increasing the growth rate from 0.163 µm/h to 291 µm/h leads to a RMS roughness improved by a factor of two. It can be

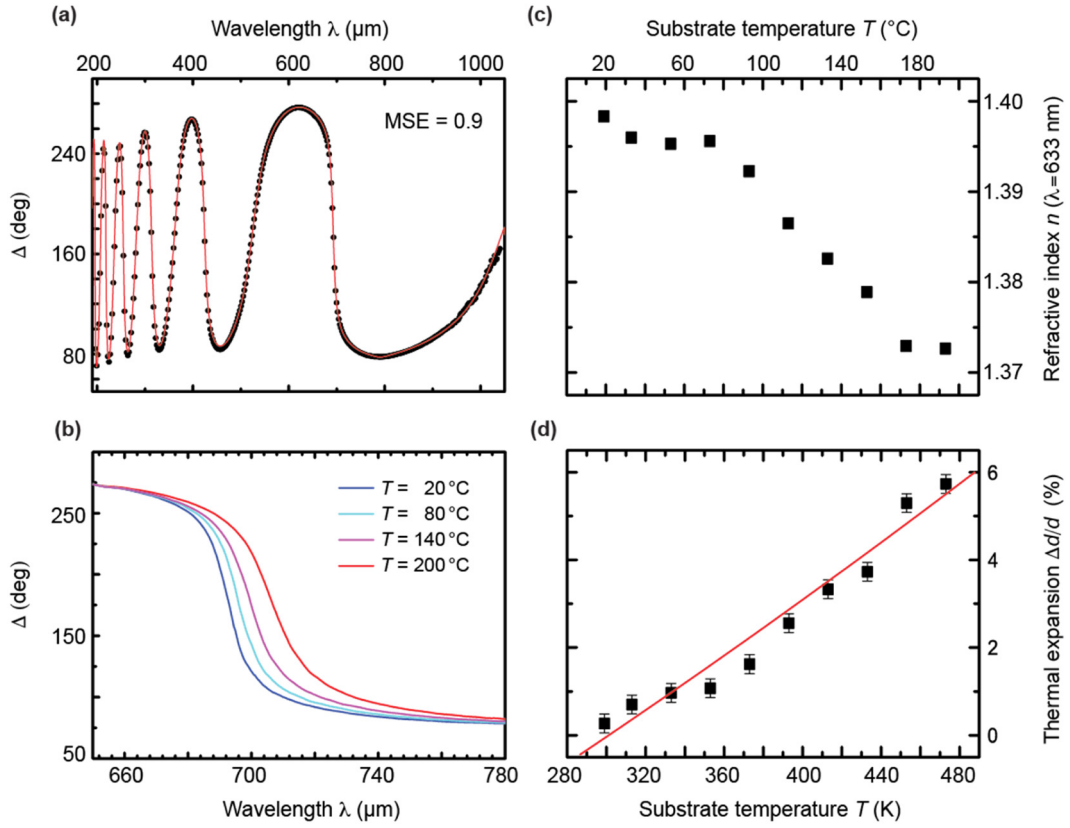

Fig. 5. The elasticity of (sub-)micrometer-thin PDMS membranes based on thermal expansion detected by spectroscopic ellipsometry. (a) The proposed model (red-colored line) of the optical properties of a 0.5 µm-thin PDMS film on the Si(111)-wafer with a 2.5 nm-thin native SiO_2 matches the obtained spectroscopic Δ-spectrum (circles). A mean square error (MSE) of 0.9 is obtained based on a Tauc-Lorentz dispersion formula [13]. (b) The shift of the spectroscopic Δ-data with substrate temperature T (blue- to red-colored curves, respectively) is presented for the wavelengths λ between 650 and 780 nm. (c) The extracted refractive index n and (d) the thermal expansion $\Delta d/d$ of the film thickness d is shown for substrate temperatures between 20 and 200 °C, 293 and 473 K, respectively. A polynomial fit (red-colored line) describes the thermal expansion based on the increase of film thickness with increasing temperature [25,26] while the refractive index n decreases.

reasonably assumed that the reduced density of radicalized functional groups per PDMS molecule induces an enhanced mobility on the surface. Reducing the growth rates below 0.163 μm/h, the RMS roughness seem to stay constant. Instead, we do observe ordered structures with a wrinkle wavelength of a few hundred nanometers. We hypothesize that the wrinkle formation is the result of the UV irradiation at low growth rates. Here, the application of thermal energy heats the surface and generates a temperature gradient towards the substrate. This thermal stress increases with film thickness and is released *via* wrinkles [5,30]. Obviously, the phenomenon is more critical the thinner the membrane. The preferential orientation of the wrinkles is due to the oblique *in situ* UV light irradiation with an incident angle of 20° to the substrate normal. Such a preferential orientation of organic molecules has been shown for oblique-incidence molecular beam deposition [31]. We reasonably assume that the anisotropic thermal irradiation causes a gradient in cross-linking densities, which leads to the directional stress release as reported in directional plasma treatments of polymer surfaces [32,33]. Consequently, PDMS membranes of highest quality require the highest possible temperatures in the evaporation sources. In order to tailor the surface morphology of the PDMS membranes with desired wrinkled structures, we propose, UV treatments at oblique incidence. Detailed studies with well selected angles of incidence are necessary to optimize the size, shape and orientation of the wrinkles.

More than 90% of the UV light with wavelengths below 190 nm is absorbed within the top 100 nm of the PDMS membrane [16,34]. Therefore, the thermal evaporation of vinyl-functionalized PDMS combined with *in situ* UV irradiation of a deuterium lamp leads to homogenous cross-linking within the membrane [35].

The elastic moduli decrease with increasing growth rates. The longer the UV radiation acts on the growing PDMS film the more functional vinyl groups and methyl side groups will be radicalized and bonded. Thus, we can correlate the maximum elastic modulus of (608 ± 9) MPa to a porous network of residual Si-O backbones – comparable to that of a porous silica-like network with a porosity of 93% [36]. Given by the thermal stability of vinyl groups [11] and our experimental setup, the maximal growth rate of 0.42 μm/h led to a minimal elastic modulus of (560 ± 150) kPa for 0.5 μm-thin membranes. These experimental results require a UV irradiation and fabrication time of about 1.2 h. To further reduce the cross-linking and thus, to realize an elastic modulus similar to human soft tissues, a pulsed UV treatment is proposed.

AFM nano-indentations have been employed as a standard technique to determine the elastic properties of polymer thin films [37]. SE is complementary to AFM: First, it allows for non-invasive measurements and second, the measurement spot allows for the characterization over macroscopic areas, here based on an $4 \times 10\ mm^2$-sized spot. The shift of the dielectric function as the function of the substrate temperature permits the determination of the thermal expansion coefficient of substrate-fixed PDMS membranes, as displayed in Fig. 5 for cross-linked 0.5 μm-thin membranes ($G = 160$ nm/h, $T = 250$ °C). The thermal expansion coefficient vertically to the substrate surface of $(2.85 \pm 0.19)\ 10^{-4}\ K^{-1}$ at room temperature corresponds well to one third of the volumetric thermal expansion coefficient of $9 \times 10^{-4}\ K^{-1}$ presented in literature [25]. AFM nano-indentations reveal the corresponding elastic modulus of (3.5 ± 0.1) MPa. Based on the generalized expansibility-theory for amorphous materials found by R.E. Baker et al. [38], one class of materials obeys a constant α - E relation. For *in situ* UV-cured, linear-chain-based PDMS networks the resulting $E\alpha^2$ - product is $(0.25 \pm 0.08)\ PaK^{-2}$. Future work will be invested to study the influence of the membrane thickness on this ratio, as the substrate effects have to be considered for both, the AFM nano-indentations as well as for the results of SE. Due to the linking of the PDMS membrane to the SiO_2 substrate surface an anisotropic thermal expansion, preferentially vertical to the substrate surface, has to be considered. This phenomenon may result in an overestimation of the detected thermal expansion coefficient und thus an underestimation of the elastic modulus by SE. Contrary, AFM nano-indentations on 0.5 μm-thin membranes may overestimate the elastic modulus due to substrate effects, see Fig. 4b. However, the preliminary data set highlights the possibility of spectroscopic ellipsometry to characterize the expansibility of substrate-fixed polymer (sub-)micrometer-thin membranes. Based on future extensive SE-AFM calibration data the $E\alpha^2$ - relation will allow extracting the elasticity of these thin films *in situ*.

5. Conclusion

In this study, we demonstrate the capability of organic molecular beam deposition to realize sub-micrometer thin PDMS films with a RMS surface roughness well below 10 nm. The 0.5 μm-thin membranes, which exhibit a peak-to-valley height difference of only a few nanometers, perfectly fit the requirements of low-voltage dielectric elastomer transducers. The elasticity of the three-dimensionally cross-linked polymer films corresponds to a few hundred kPa and is, therefore, comparable to the mechanical properties of human soft tissue [14,17]. As a consequence, these thin films form a sound basis for artificial skin and artificial muscles [39]. The AFM and *in situ* SE are complementary techniques to thoroughly characterize the elasticity and the morphology of these thin films [12].

Acknowledgements

The financial contributions of the Swiss National Science Foundation (Bridge-Proof of concept project 20B1-1_175197), and of the Swiss Nanoscience Institute (SNI) for the AFM, is gratefully acknowledged.

References

[1] E. Ozbay, Science 311 (5758) (2006) 189–193.
[2] T. Töpper, S. Lörcher, H. Deyhle, B. Osmani, V. Leung, B. Müller, Adv. Elec. Mat. 3 (8) (2017) 1700073.
[3] R.T. Hill, Wiley Interdiscip. Rev. Nanomed. Nanobiotechnol. 7 (2) (2015) 152–168.
[4] J.A. Rogers, T. Someya, Y. Huang, Science 327 (5973) (2010) 1603–1607.
[5] B. Osmani, T. Töpper, H. Deyhle, T. Phohl, B. Müller, Adv. Mat. Tech. 2 (10) (2017) 1700105.
[6] B. Osmani, H. Deyhle, F.M. Weiss, T. Töpper, M. Karapetkova, V. Leung, B. Müller, Proc. SPIE 9798 (2016) 979822.
[7] T. Töpper, F.M. Weiss, B. Osmani, C. Bippes, V. Leung, B. Müller, Sensors Actuators A Phys. 233 (2015) 32–41.
[8] G.G. Arthur, B.J. McKeon, S.S. Dearing, J.F. Morrison, Z. Cui, Microelectron. Eng. 83 (4) (2006) 1205–1208.
[9] J.C. McDonald, G.M. Whitesides, Acc. Chem. Res. 35 (7) (2002) 491–499.
[10] F.B. Madsen, A.E. Daugaard, S. Hvilsted, A.L. Skov, Macromol. Rapid Commun. 37 (5) (2016) 378–413.
[11] T. Töpper, S. Lörcher, F.M. Weiss, B. Müller, APL Mater. 4 (5) (2016) 056101.
[12] F.M. Weiss, F.B. Madsen, T. Töpper, B. Osmani, V. Leung, B. Müller, Mater. Des. 105 (2016) 106–113.
[13] H. Fujiwara, Spectroscopic Ellipsometry: Principles and Applications, John Wiley & Sons, 2007.
[14] X. Liang, S.A. Boppart, IEEE Trans. Biomed. Eng. 57 (4) (2010) 953–959.
[15] H.F. Mark, Encyclopedia of Polymer Science and Technology, Vol. 15, Wiley & Sons, New York, 2014.
[16] T. Töpper, F. Wohlfender, F. Weiss, B. Osmani, B. Müller, Proc. SPIE 9798 (2016) 979821.
[17] R. Akhtar, M.J. Sherratt, J.K. Cruickshank, B. Derby, Mater. Today 14 (3) (2011) 96–105.
[18] S. Guo, I. Lundström, H. Arwin, Appl. Phys. Lett. 68 (14) (1996) 1910–1912.
[19] O. Kahle, U. Wielsch, H. Metzner, J. Bauer, C. Uhlig, C. Zawatzki, Thin Solid Films 313 (Supplement C) (1998) 803–807.
[20] B. Osmani, S. Seifi, H.S. Park, V. Leung, T. Töpper, B. Müller, Appl. Phys. Lett. 111 (9) (2017), 093104. .
[21] C. Dölle, M. Papmeyer, M. Ott, K. Vissing, Langmuir 25 (12) (2009) 7129–7134.
[22] J.E. Sader, J.W.M. Chon, P. Mulvaney, Rev. Sci. Instrum. 70 (10) (1999) 3967–3969.
[23] F. Carrillo, S. Gupta, M. Balooch, S.J. Marshall, G.W. Marshall, L. Pruitt, C.M. Puttlitz, J. Mater. Res. 20 (10) (2005) 2820–2830.
[24] Y.M. Efremov, D.V. Bagrov, M.P. Kirpichnikov, K.V. Shaitan, Colloids Surf. B: Biointerfaces 134 (2015) 131–139.
[25] A.C.M. Kuo, Polymer Data Handbook, Oxford University Press, 1999.
[26] H. Shih, P.J. Flory, Macromolecules 5 (6) (1972) 758–761.
[27] D.F. Wilcock, J. Am. Chem. Soc. 68 (4) (1946) 691–696.
[28] B. Müller, L. Nedelmann, B. Fischer, H. Brune, J.V. Barth, K. Kern, D. Erdös, J. Wollschläger, Surf. Rev. Lett. 5 (1998) 769–781.

[29] Y. Israëli, J. Cavezzan, J. Lacoste, Polym. Degrad. Stab. 37 (3) (1992) 201–208.
[30] B. Osmani, G. Gerganova, B. Müller, Eur. J. Nanomed. 9 (2) (2017) 69–77.
[31] B. Müller, C. Cai, A. Kündig, Y. Tao, M. Bösch, M. Jäger, P. Günter, Appl. Phys. Lett. 74 (21) (1999) 3110–3112.
[32] J.S. Lee, H. Hong, S.J. Park, S.J. Lee, D.S. Kim, Microelectron. Eng. 176 (Supplement C) (2017) 101–105.
[33] J. Genzer, J. Groenewold, Soft Matter 2 (4) (2006) 310–323.
[34] N.E. Stankova, P.A. Atanasov, R.G. Nikov, N.N. Nedyalkov, T.R. Stoyanchov, N. Fukata, K.N. Kolev, E.I. Valova, J.S. Georgieva, S.A. Armyanov, Appl. Surf. Sci. 374 (Supplement C) (2016) 96–103.
[35] T. Töpper, B. Osmani, S. Lörcher, B. Müller, Proc. SPIE 10163 (2017) 101631F.
[36] D. Bellet, P. Lamagnère, A. Vincent, Y. Bréchet, J. Appl. Phys. 80 (7) (1996) 3772–3776.
[37] D. Tranchida, S. Piccarolo, M. Soliman, Macromolecules 39 (13) (2006) 4547–4556.
[38] J.R.E. Barker, J. Appl. Phys. 34 (1) (1963) 107–116.
[39] E. Fattorini, T. Brusa, C. Gingert, S.E. Hieber, V. Leung, B. Osmani, M.D. Dominietto, P. Büchler, F. Hetzer, B. Müller, Ann. Biomed. Eng. 44 (5) (2016) 1355–1369.